

RESEARCH

Open Access



# De novo biosynthesis of $\beta$ -Arbutin in *Komagataella phaffii* based on metabolic engineering strategies

Jiashuo Yang<sup>1</sup>, Liu Yang<sup>1</sup>, Fengguang Zhao<sup>1</sup>, Chunting Ye<sup>1</sup> and Shuangyan Han<sup>1\*</sup>

## Abstract

**Background**  $\beta$ -Arbutin, found in the leaves of bearberry, stands out as one of the globally acknowledged eco-friendly whitening additives in recent years. However, the natural abundance of  $\beta$ -Arbutin is low, and the cost-effectiveness of using chemical synthesis or plant extraction methods is low, which cannot meet the requirements. While modifying the  $\beta$ -Arbutin synthesis pathway of existing strains is a viable option, it is hindered by the limited synthesis capacity of these strains, which hinders further development and application.

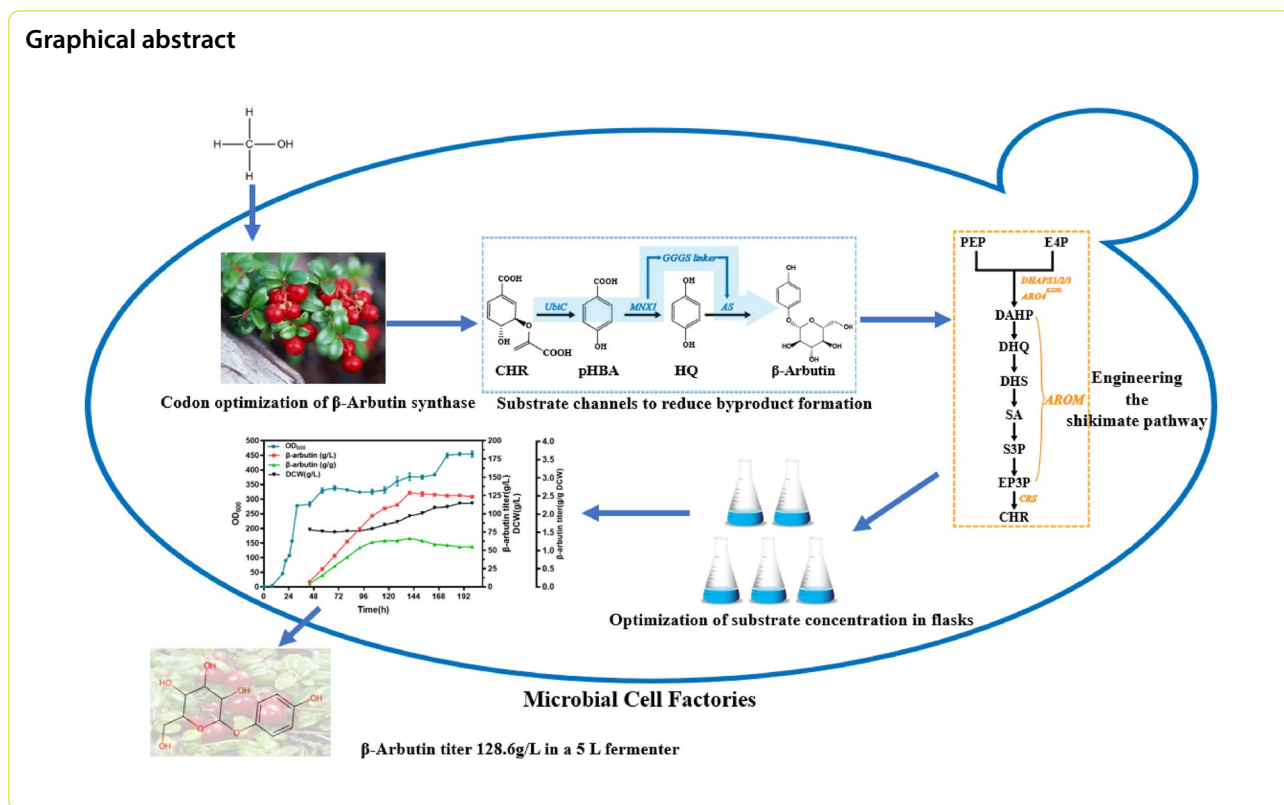
**Results** In this study, we established a biosynthetic pathway in *Komagataella phaffii* for  $\beta$ -Arbutin production with a titer of 1.58 g/L. Through diverse metabolic strategies, including fusion protein construction, enhancing shikimate pathway flux, and augmenting precursor supplies (PEP, E4P, and UDPG), we significantly increased  $\beta$ -Arbutin titer to 4.32 g/L. Further optimization of methanol concentration in shake flasks led to a titer of 6.32 g/L titer after 120 h of fermentation, representing a fourfold increase over the initial titer. In fed-batch fermentation, strain UA3-10 set a record with the highest production to date, reaching 128.6 g/L in a 5 L fermenter.

**Conclusions** This is the highest yield in the fermentation tank level of using microbial cell factories for de novo synthesis of  $\beta$ -Arbutin. Applying combinatorial engineering strategies has significantly improved the  $\beta$ -Arbutin yield in *K. phaffii* and is a promising approach for synthesizing functional products using a microbial cell factory. This study not only advances low-cost fermentation-based production of  $\beta$ -Arbutin but also establishes *K. phaffii* as a promising chassis cell for synthesizing other aromatic amino acid metabolites.

**Keywords** *K. phaffii*,  $\beta$ -Arbutin, Shikimate pathway, Methanol, Metabolic strategies

\*Correspondence:  
Shuangyan Han  
syhan@scut.edu.cn





## Background

$\beta$ -Arbutin, naturally present in the leaves of various plants, is now widely used as a skin-whitening agent in cosmetic industries because of its inhibitory effect on tyrosinase, an important enzyme for generating melanin pigments [1]. Beyond its established role as a whitening agent,  $\beta$ -Arbutin also demonstrates antibacterial properties [2] and anti-inflammatory attributes [3]. Many brands are increasingly focusing on utilizing gentle yet effective ingredients to meet market demand. Furthermore, a growing number of studies and experiments have demonstrated the efficacy of  $\beta$ -Arbutin and its safety within the realms of beauty and skincare, accelerating the research and market introduction of related products. Consumers' emphasis on skincare effectiveness, ingredient safety, and user experience has led to a rising popularity of products containing  $\beta$ -Arbutin, thus stimulating market demand. Previously,  $\beta$ -Arbutin was mainly extracted from plants, resulting in low yield and difficulty in purification [4], which has led to a loss of competitiveness amid increasing market demand. Chemical synthesis of  $\beta$ -Arbutin, based mostly on the Helderich method, employed the toxic hydroquinone (HQ), exhibiting low isomer selectivity, harsh conditions, and inefficiency [5]. Thus, more regioselectivity, mild condition, and environment-friendly

biosynthesis of  $\beta$ -Arbutin production are more favored by the cosmetic industry.

One-pot biocatalytic production of  $\beta$ -Arbutin from exogenous HQ without protection/deprotection steps has also been explored and adopted by some researchers. Nevertheless, the transversion require the use of HQ, which in turn is produced industrially by a multi-step chemical process that is hardly considered a green technique. In response to these concerns, current researchers shifted focus to microbial cell de novo synthesis to produce of  $\beta$ -Arbutin [4]. De novo synthesis in microbial cell factory can start with glucose, glycerol, or other simply carbon sources, bypassing the laborious chemical methods and circumventing the direct involvement of HQ, while maintaining the catalytic specificity and efficiency [5]. Moreover, in comparison to plant extraction, utilizing microorganisms to produce  $\beta$ -Arbutin is equally environmentally friendly and demonstrates higher production efficiency. Using the extraction of  $\beta$ -Arbutin from pear leaves as an example [6], the maximum yield of  $\beta$ -Arbutin using water extraction and organic solvent extraction were 14.3 mg/g and 12.3 mg/g, respectively. In contrast, when producing  $\beta$ -Arbutin through microorganisms at the bioreactor level, production rates can reach several tens grams per liter [7]. Furthermore, microbial production of  $\beta$ -Arbutin is not influenced by seasonal factors.

Some cases of applying cell factories constructed through metabolic engineering approaches toward the production of  $\beta$ -Arbutin in recent years to produce  $\beta$ -Arbutin are summarized and listed in Table 1. However, the productivity of these traditional industrial strains is somewhat limited. Furthermore,  $\beta$ -Arbutin could be achieved via fermentation using engineering high-performance strains, which offer significant advantages in scaling up production.

One of the characteristics of microbial fermentation is its ability to utilize cost-effective and renewable raw materials through microbial metabolism, thereby alleviating the dependence on fossil fuels. However, traditional industrial fermentation feedstocks derived from sugar-based sources like sugar cane and maize pose challenges such as competing for food, elevating food costs, and limitations related to arable land availability [8]. Methanol is an ideal feedstock owing to its low price, abundance, higher degree of reduction, energy density, and ease of storage and transport [9]. It could be produced from CO<sub>2</sub> and hydrogen (electrolysis of water) by photocatalysis or electrocatalysis, significantly increasing competitiveness of methanol biomanufacturing [10]. *Komagataella phaffii*, which uses the C1 compound methanol as its sole energy and carbon source, has been widely used to produce heterologous proteins for the biopharmaceutical and enzyme markets [11]. *K. phaffii* offers several advantages: (1) It represents a straightforward eukaryotic expression system which, in contrast to prokaryotic systems, boasts a wide array of post-translational modification mechanisms while lacking endotoxin production [12]. (2) The AOX1 promoter, strictly regulated by methanol, enables selective induction of specific gene expression, facilitating better regulation of cellular physiological activities during fermentation compared to constitutive promoters [13]. (3) It is a Crabtree-negative strain that achieves high-density fermentation without ethanol production under aerobic conditions [13], thriving in a pH range of approximately 3.0–7.0, which is advantageous for large-scale fermentation processes. (4) Its genetic background

is well characterized, with detailed annotations of the genome sequencing results of its commercial variant strain GS115 [14, 15]. The maturity of gene editing technologies, such as CRISPR/Cas9 [16], has further advanced the engineering design strategies for *K. phaffii*. Given its distinctive advantages, *K. phaffii* stands out in the biomanufacturing of  $\beta$ -Arbutin.

It is now considered to be a promising chassis host for metabolic engineering, and some well-established model for producing high-value biochemical products has been elucidated, benefiting from its high fermentation density and Generally Recognized As Safe (GRAS) [17].

In this study, we systematically engineered a *K. phaffii* host for  $\beta$ -Arbutin production (Fig. 1). The de novo synthesis of  $\beta$ -Arbutin in *K. phaffii* was achieved by introducing and optimizing the heterologous chorismate lyase *UbiC* [18], 4-hydroxybenzoate 1-hydroxylase *MNX1* [19] and hydroquinone glucosyltransferase *AS* [20]. We also extensively reprogrammed the metabolism of yeast from methanol to  $\beta$ -Arbutin, including (1) fusion overexpression of *MNX1* and *AS*. (2) amplification of the metabolic flux of the shikimate pathway, (3) improvement of precursor supply including PEP, E4P, and glucose donor UDPG, and (4) optimization of methanol concentration in the daily feedstock. Finally, the engineered *K. phaffii* was employed in fed-batch fermentation in a 5 L fermenter and the yield of  $\beta$ -Arbutin was assayed. This endeavor described here offers strategies for converting methanol to  $\beta$ -Arbutin in cell factory, which should also benefit the production of other chemicals from methanol.

## Materials and methods

### Strains and plasmids

Strains and plasmids utilized in this study are summarized in Table S1. *K. phaffii* GS115 ( $\Delta$ HIS4, Life Technologies) was used as the chassis cell for all manipulations. *E. coli* TOP10F' (Invitrogen, Carlsbad, CA, USA) was used for plasmid construction and amplification. All primers used in this study were provided by Tsingke (Beijing, China). Endogenous genes were amplified

**Table 1** Capabilities of traditional industrial microorganisms for the production of  $\beta$ -Arbutin in recent years

Product	Host	Carbon source	Fermentation duration (h)	Flask fermentation titer (g/L)	Fermenter titer (g/L)	References
$\beta$ -Arbutin	<i>E. coli</i> BL21Star (DE3)	Glucose	48	4.19		[21]
	<i>P. chlororaphis</i> P3	Glucose	72	6.79		[22]
	<i>Y. lipolytica</i>	Glucose	144	8.6		[4]
	<i>E. coli</i> BW25113	Glycerol	72	7.91	28.1	[7]
	<i>E. coli</i> BW25113	Glucose	72	3.24	43.79	[23]

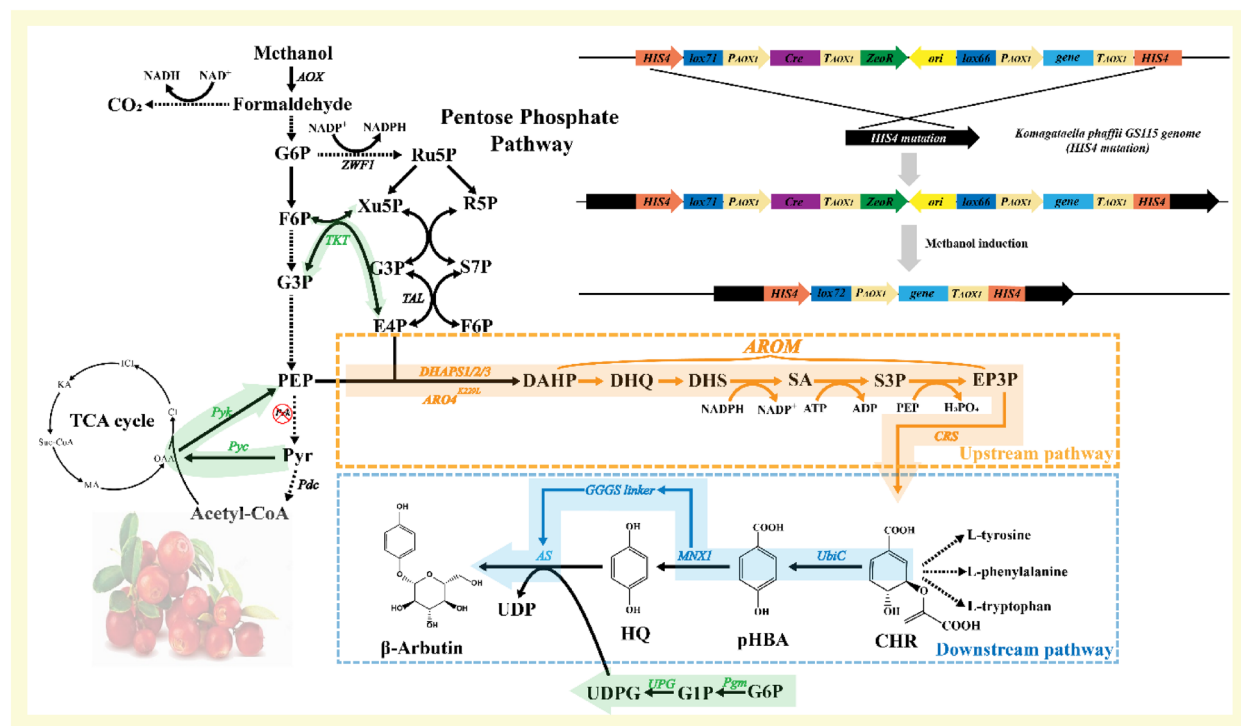


**Fig. 1** De novo biosynthesis pathway of  $\beta$ -Arbutin in *Komagataella phaffii* based on metabolic engineering strategies. G6P, glucose 6-phosphate; F6P, fructose-6-phosphate; G3P, glyceraldehyde 3-phosphate; Ru5P, ribulose 5-phosphate; Xu5P, xylulose 5-phosphate; R5P, ribose 5-phosphate; S7P, sedoheptulose 7-phosphate; E4P, erythrose 4-phosphate; PEP, phosphoenolpyruvate; Pyr, pyruvate; OAA, oxaloacetate; Ci, citric acid; ICI, isocitric acid; KA, ketoglutaric acid; Suc-CoA, succinyl coenzyme A; MA, malic acid; DAHP, 3-deoxy-D-arabinoheptulosonate 7-phosphate; DHQ, 3-dehydroquinone; DHS, 3-Dehydroshikimate; SA, shikimate; S3P, Shikimate 3-phosphate; EP3P, Emphasis>O5-(1-Carboxyvinyl)-3-phosphoshikimate; CHR, Chorismate; pHBA, p-hydroxybenzoic acid; HQ, hydroquinone; G1P, glucose 1-phosphate; UDPG, UDP-glucose; UDP, Uridine diphosphate; AOX, methanol oxidase; ZWF1, glucose 6-phosphate dehydrogenase; TKT, transketolase; TAL, transaldolase; Pyc, pyruvate carboxylase; Pyk, phosphoenolpyruvate carboxylase; Prk, pyruvate kinase; Pdc, pyruvate dehydrogenase component; DHAPS1/2/3, 3-deoxy-7-phosphoheptulonate synthase 1/2/3; ARO4<sup>K229L</sup>, 3-deoxy-7-phosphoheptulonate synthase from *Saccharomyces cerevisiae*, the 229th amino acid in which sequence mutated from leucine to lysine. AROM, pentafunctional AROM polypeptide; CRS, chorismate synthase; UbiC, chorismate lyase; MNX1, 4-hydroxybenzoate 1-hydroxylase; AS, arbutin synthase; Pgm, phosphoglucomutase; UPG, glucose-1-phosphate uridylyltransferase. The red “ $\otimes$ ” mark indicates deletion of *Prk*. Green, orange and blue coloured genes are overexpressed with plasmids from cre loxP series

from the GS115 genome. The exogenous genes, *UbiC* (NC\_000913.3), *MNX1* (CCE40241.1), *AS* (AJ310148.1), *xfpk*(KND53308.1) and *PTA* (WP\_012101779.1) were codon-optimized and synthesized by Tsingke (Beijing, China). Fragments were amplified through PCR using KOD DNA polymerase (TOYOBO, Japan) and KOD neo DNA polymerase (TOYOBO, Japan). Cloning was performed using the Gibson assembly method [24]. Transformation of yeast was achieved by electroporation using lithium acetate [25].

### Construction of yeast strain

The Cre/loxP ZeoR marker recycling method was used to construct the recombinant yeast strain [26]. The procedure for zeocin resistance knockout was as follows: The transformed yeast strain was picked and subjected to resistance knockout by inoculating it in 10 mL of BMMY medium, incubated at 30 °C on a shaker at 250 rpm for

72 h. Subsequently, streaking was performed on YPD agar plates and incubated at 30 °C for 48 h. YPD and YPDZ plates were used to verify the resistance knockout of the same transformant. A successful resistance knockout was indicated if the colonies grew normally on YPD plates but not on YPDZ plates. The *UbiC*, *MNX1*, *AS*, and the *MNX1-GGGs-AS* were integrated at the *HIS4* locus [26], while the remaining genes were integrated at the *int1* locus [27].

### Shake flask cultures and conditions

*E. coli* Top10 F' was cultured in LB medium (5 g/L yeast extract, 10 g/L tryptone, and 10 g/L NaCl) or low salt LBL medium (5 g/L yeast extract, 10 g/L tryptone, and 5 g/L NaCl) with the addition of 100  $\mu$ g/mL zeocin for the amplification of recombinant plasmids at a temperature of 37 °C. Recombinant yeast strains were cultivated in either YPD (10 mL and 100 mL), or in 10 mL BMGY

and 25 mL BMMY medium. YPD medium consisted of 2% peptone, 2% glucose, and 1% yeast extract. BMGY medium contained 2% peptone, 1.34% YNB, 1% yeast extract, 0.1 mM potassium phosphate buffer with pH 6.0, and 1% glycerol. BMMY medium contains 2% peptone, 1.34% YNB, 1% yeast extract, 0.1 mM potassium phosphate buffer with pH 6.0, and 1% methanol per day. The yeast seed cultures were initially inoculated into 10 mL of BMGY medium in a 50 mL flask and grown for 24 h at 30 °C in a shaking incubator at 250 rpm. Subsequently, the main cultures were inoculated into a 250 mL flask containing 25 mL of BMMY medium with an initial OD<sub>600</sub> of 0.2 or 1, and cultured in a shaking incubator under the same conditions for 120 h.

#### Characterization and quantification of $\beta$ -Arbutin

Standard  $\beta$ -Arbutin was purchased from Macklin ( $\geq 98\%$ ) and subjected to characterization using UPLC-MS/MS, while quantification was performed using HPLC. Characterization of  $\beta$ -Arbutin was carried out according to a previously reported method [28]. The appropriate fermentation broth was centrifuged at 5500 $\times$ g for 5 min and the supernatant was collected. For quantification, the titer of  $\beta$ -Arbutin, samples were analyzed by HPLC on a C18 column (Synergi™ 4  $\mu$ m Hydro-RP80, Aphenomenex). Mobile phase [29]: water–methanol (90:10); flow rate: 1.0 mL/min; column temperature: 25°C; detection wavelength: 282 nm; injection volume: 20  $\mu$ L. Under the chromatographic conditions, the baseline separation of  $\beta$ -Arbutin could be achieved (Figure S1).

#### Fed-batch fermentation for the production of $\beta$ -Arbutin

The 2L BSM medium in the high-density fermentation contained 4% glycerol, 0.093% CaSO<sub>4</sub>·2H<sub>2</sub>O, 1.147% MgSO<sub>4</sub>, 1.82% K<sub>2</sub>SO<sub>4</sub>, 0.413% KOH, 2.67% H<sub>3</sub>PO<sub>4</sub>, and 0.435% PTM1. The trace metal solution PTM1 containing 0.05% CoCl<sub>2</sub>·6H<sub>2</sub>O, 0.6% CuSO<sub>4</sub>·5H<sub>2</sub>O, 6.5% FeSO<sub>4</sub>·7H<sub>2</sub>O, 0.002% H<sub>3</sub>BO<sub>3</sub>, 0.008% NaI, 0.5% H<sub>2</sub>SO<sub>4</sub>, 0.02% Na<sub>2</sub>MoO<sub>4</sub>·2H<sub>2</sub>O, 2% ZnCl<sub>2</sub>, 0.3% MnSO<sub>4</sub>·H<sub>2</sub>O, and 0.02% biotin, was used in the cultivation. A UA3-10 single colony was first inoculated into a 50 mL Erlenmeyer flask containing 10 mL of YPD medium at 30 °C in shaking incubator at 250 rpm for approximately 24 h. Subsequently, 4% of the seed culture was transferred to a 500 mL Erlenmeyer flask containing 160 mL of YPD medium and cultured under the same conditions for approximately 20 h. Finally, the whole seed culture was inoculated into a 2 L BSM medium in a 5 L fermenter for fed-batch fermentation (FUS10-A, Shanghai Guoqiang Bioengineering Equipment, Shanghai, China).

The fermentation process was divided into three stages. The initial stage was carried out in BSM medium (initial BSM medium with the addition of 8.7 mL PTM1). The

temperature was controlled at 30 °C and pH was maintained at 5.5 by continuously adding ammonia water in real-time. The glycerol in the medium depleted in approximately 18–24 h, leading to a dissolved oxygen rebound, marking the transition to the second fermentation stage. Temperature and pH conditions remained consistent with the first stage. Limited glycerol was supplemented at a reduced rate (6 mL PTM1 per 500 mL glycerol) to slow down cell growth until an OD<sub>600</sub> of 250–300 was achieved. Following on, glycerol feeding was stopped, and the next stage began after complete depletion of the glycerol. The third stage is the methanol induction stage, where methanol is the carbon source in the medium (12 mL PTM1 per liter methanol). The temperature was adjusted to 25 °C, the pH was set to 6.0, and the speed gradually increased to 1000–1200 rpm. The initial methanol feeding rate was 4 g/L/h, which was adjusted in real-time. Methanol feeding was stopped intermittently to observe changes in dissolved oxygen. If a dissolved oxygen rebound was observed within half a minute, it indicated that methanol had not accumulated and the methanol feeding rate could be further increased. Dissolved oxygen (DO) was stabilized between 20% and 30%, and the airflow rate was gradually increased from 4 to 8 L/min according to the dissolved oxygen. OD<sub>600</sub> and  $\beta$ -Arbutin production were measured every 12 h. The duration of the methanol induction phase lasted for 144 h.

## Results and discussion

### Construction and optimization of the heterologous $\beta$ -Arbutin production pathway

According to the literature [21], chorismate can be converted into  $\beta$ -Arbutin through three enzymes: chorismate lyase (*UbiC*) can transform chorismate into *p*-hydroxybenzoic acid (pHBA) while 4-hydroxybenzoate 1-hydroxylase (*MNX1*) and hydroquinone glucosyltransferase (*AS*) are involved in decarboxylation of pHBA to hydroquinone (HQ) and its subsequent glycosylation into  $\beta$ -Arbutin. Since *K. phaffii* naturally possesses a shikimate pathway capable of supplying chorismate, introducing this pathway artificially could enable the production of  $\beta$ -Arbutin in *K. phaffii*.

We introduced these three heterologous enzymes into *K. phaffii* and verified their functions (data not shown). Subsequently, all enzymes were introduced into *K. phaffii*, and analysis of  $\beta$ -Arbutin were conducted on the fermentation supernatant. As shown in the HPLC analysis chromatogram, a new peak with a retention time of 4.7 min appeared in our engineered strain, aligns with the retention time of the standard whereas the control did not (Figure S1). The titer of  $\beta$ -Arbutin and OD<sub>600</sub> of the strain UA1-1 were detected in the whole fermentation

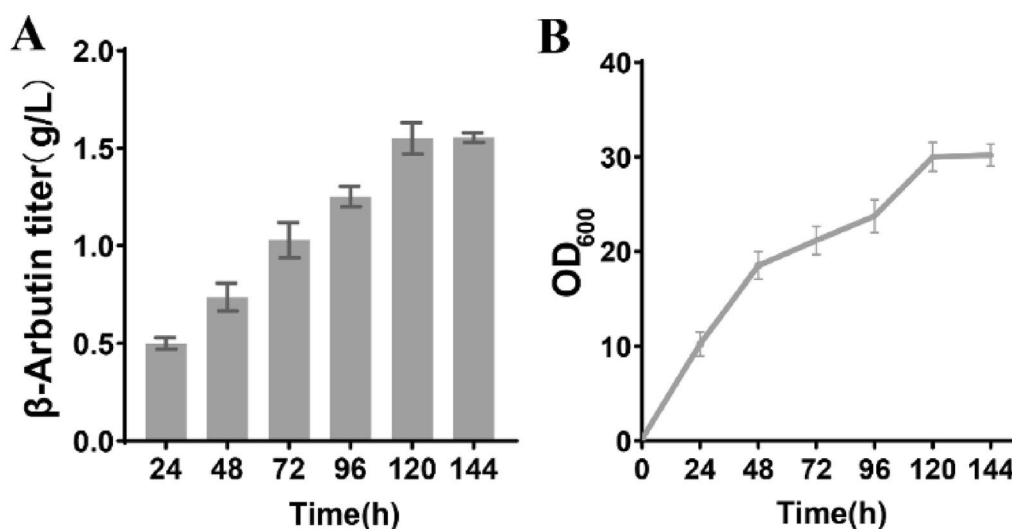


**Fig. 2** De novo synthesis of  $\beta$ -Arbutin in engineered *K. phaffii*. **A**  $\beta$ -Arbutin titer of the strain UA1-1. **B** Growth curves of the strain UA1-1. Data are presented as mean from triplicate experiments

period, revealing an accumulation of 1.57 g/L  $\beta$ -Arbutin at 120 h (Fig. 2A, B). Since the production reached a steady state after 120 h, we chose to use 120 h as the cycle for subsequent fermentation process. In addition, we also conducted fed-batch fermentation on UA1-1 and achieved an initial  $\beta$ -Arbutin yield of 68.02 g/L (Figure S2), demonstrating the production capability of the initial strain.

In multi-step biosynthetic pathways, the titer of the target compound can be affected by losses of intermediates, which may occur due to diffusion, oxidation and other factors. To improve the conversion rate of target compound, consecutive enzymes can be expressed as fusion with linker regions [30, 31]. In  $\beta$ -Arbutin pathway, it was observed that the intermediate HQ was prone easy oxidation. During fermentation, we observed a gradual darkening of the medium, coinciding with the color of *p*-benzoquinone (the oxidation product of HQ). We hypothesized that this transformation could negatively affect the synthesis efficiency of  $\beta$ -Arbutin. Therefore, we employed substrate channels through fusion of *MNX1* and *AS* using peptide linker GGGs. To this end, the fusion of *MNX1* and *AS* with linker GGGs was achieved using distinct sequence orders (Fig. 3A). Fermentation was then conducted to compare the differences in  $\beta$ -Arbutin yield among UA1-1, UA2-1, and UA2-2. A  $\beta$ -Arbutin concentration of 1.88 g/L was obtained in UA2-1, resulting in a 19.7% improvement compared to UA1-1 (Fig. 3B). To validate our conclusion, we amplified the differences by supplementing the precursor substance *p*HBA. Specifically, 2 g/L of *p*HBA was added to the medium at 24 h of methanol

fermentation. The  $\beta$ -Arbutin titer was measured at 48 h and 72 h, as shown in Fig. 3D. At 48 h, the titer of UA2-1 was 19.7% higher than UA1-1 and it remained 12.6% higher at 72 h, demonstrating the effectiveness of the substrate channel *MNX1-GGGs-AS*. However, the titer of UA2-2 was 26.7% lower than UA1-1. Notably, the  $\beta$ -Arbutin titer of UA2-1 strain reached 3.44 g/L at 72 h, significantly surpassing the titer achieved at 120 h without *p*HBA added. This observation highlights that the insufficient supply of *p*HBA is a significant limiting factor for  $\beta$ -Arbutin production at present.

#### Engineering the shikimate pathway to improve $\beta$ -Arbutin production

The intermediate of the shikimate pathway, chorismate, is the direct precursor of *p*HBA. Our goal in this regulation was to maximize the metabolic flux of chorismate for the synthesis of  $\beta$ -Arbutin. By exploring KEGG, we identified endogenous genes involved in the biosynthesis of chorismate in *K. phaffii*, such as 3-deoxy-arabino-heptulonate 7-phosphate synthase (*DHAPS1*, Emphasis>PAS\_chr1-4\_0218; *DHAPS2*, PAS\_chr2-1\_0473; *DHAPS3*, PAS\_chr3\_0936), pentafunctional AROM polypeptide (*aroM*, PAS\_chr3\_0506) and chorismate synthase (*CRS*, PAS\_chr2-1\_0637). DHAP synthase catalyzes the condensation of E4P and PEP, representing the initial step in the shikimate pathway. Previous studies have emphasized the key role of this condensation in *Y. lipolytica* [4]. *Aro4*<sup>K229L</sup> is a DHAP synthase isoform derived from *S. cerevisiae*. Previous studies have shown that modifying specific residues can reduce the feedback inhibition of Aro4 [32]. The K229L mutation in this protein renders it insensitive to

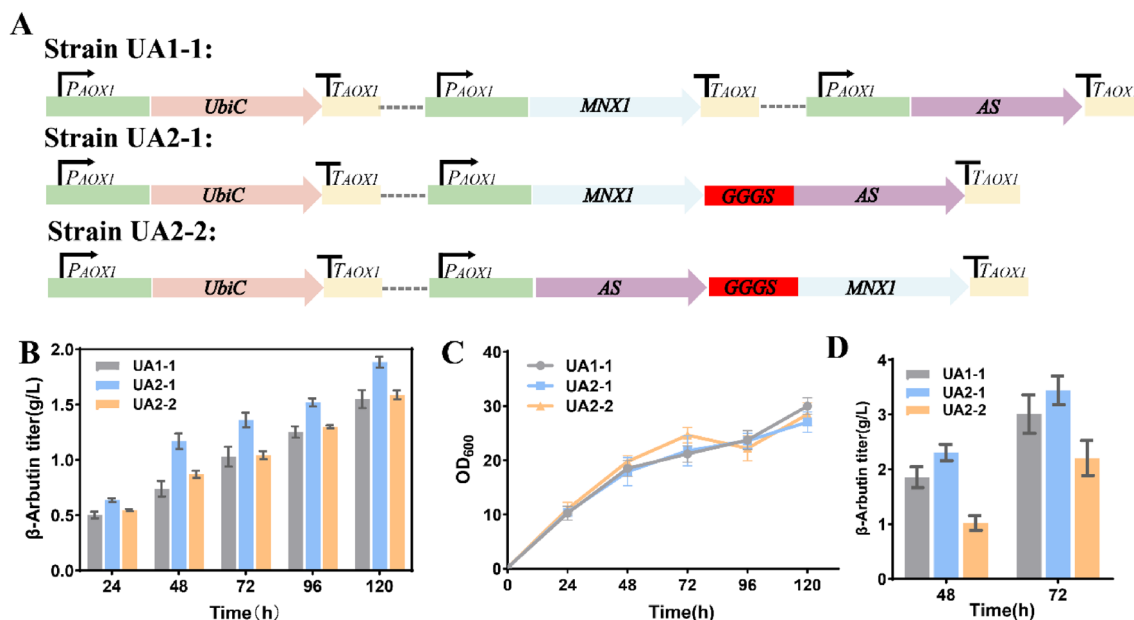


**Fig. 3**  $\beta$ -Arbutin production in *K. phaffii* overexpressing MNX1 and AS in different fusion forms. **A** Schematic diagram of UA1-1, 2-1 and 2-2. **B**  $\beta$ -Arbutin titer of the strain UA1-1, 2-1 and 2-2. **C** Growth curves of the strain UA1-1, 2-1 and 2-2. **D** The difference in  $\beta$ -Arbutin yield generated by two substrate channels and UA1-1 with 2 g/L pHBA added at 24 h. Data are presented as mean from triplicate experiments

phenylalanine and tyrosine while still maintaining overall activity. This mutation was successfully utilized in *S. cerevisiae* to enhance the production of various aromatic products [33–35]. The pentafunctional peptide AroM is known to catalyze five consecutive reactions in the shikimate pathway, serving as a natural scaffold for substrate channeling in yeast [36]. The final step of the shikimate pathway is facilitated by the chorismate synthase *CRS*. Relevant studies indicate that overexpression of *CRS* can enhance the production of *p*-coumaric acid in *S. cerevisiae* [37]. To identify enzymes with superior performance, six potential genes based on the UA2-1 strain were overexpressed, and their impact on  $\beta$ -Arbutin productivity was assessed.

For strain UA2-1, it was observed that both OD<sub>600</sub> and  $\beta$ -Arbutin titer had not reached saturation at 120 h (Fig. 2A, B), potentially influencing the differences between strains. Compared to other engineered strains of *K. phaffii* under similar culture conditions, UA2-1 exhibited an OD<sub>600</sub> of less than 30 at 120 h, significantly lower than others with an OD<sub>600</sub> of 40–50 in same timeframe [38, 39]. We hypothesized that the growth inhibition of UA2-1 could be attributed to the toxicity of *p*-benzoquinone, consequently impacting  $\beta$ -Arbutin titer. To accelerate the saturation of OD<sub>600</sub>, we adjusted the initial OD<sub>600</sub> from 0.2 to 1.0 in our fermentation. As shown in Fig. 4A, UA3-3 showed a substantial increase in  $\beta$ -Arbutin production (3.58 g/L) compared to UA2-1 (2.51 g/L), marking a 43.2% improvement. Among

the five enzymes individually overexpressed, *DHAPS3* (3.58 g/L) and *DHAPS2* (3.09 g/L) increased  $\beta$ -Arbutin production significantly. *CRS* demonstrated a 12.7% improvement (2.83 g/L) over UA2-1, *DHAPS1* showed an 8.5% increase (2.72 g/L) and *AroM* exhibited a 1.5% increase (2.54 g/L). This indicates that the condensation reaction involving *DHAPS3* serves as the rate-limiting step in the shikimate pathway in *K. phaffii*, underscoring the importance of the condensation of PEP and E4P for production of  $\beta$ -Arbutin. According to the literature, the co-expression strategy of screening pathways has proven effective in enhancing the yield of target products in *K. phaffii* [38]. Based on the above results, we combined the effective genes with *DHAPS3* to obtain optimal strains (Fig. 4A). As shown in Fig. 4A, B, although the  $\beta$ -Arbutin titer did not decrease, the overexpression of these genes imposed varying degrees of metabolic burden on the strains. These strategies did not always improve the yield in all combinations tested. However, the strain UA3-10 produced 4.32 g/L of  $\beta$ -Arbutin within 120 h, which is a substantial 72.1% increase compared to UA2-1.

#### Enrichment of the precursor PEP and E4P and UDPG pool

The de novo synthesis of  $\beta$ -Arbutin requires two precursors, E4P and PEP, derived from the PPP (pentose phosphate pathway) and glycolysis pathways. PEP participates in various pathways such as glycolysis and shikimate pathway. The initial step in shikimate pathway is the condensation between PEP

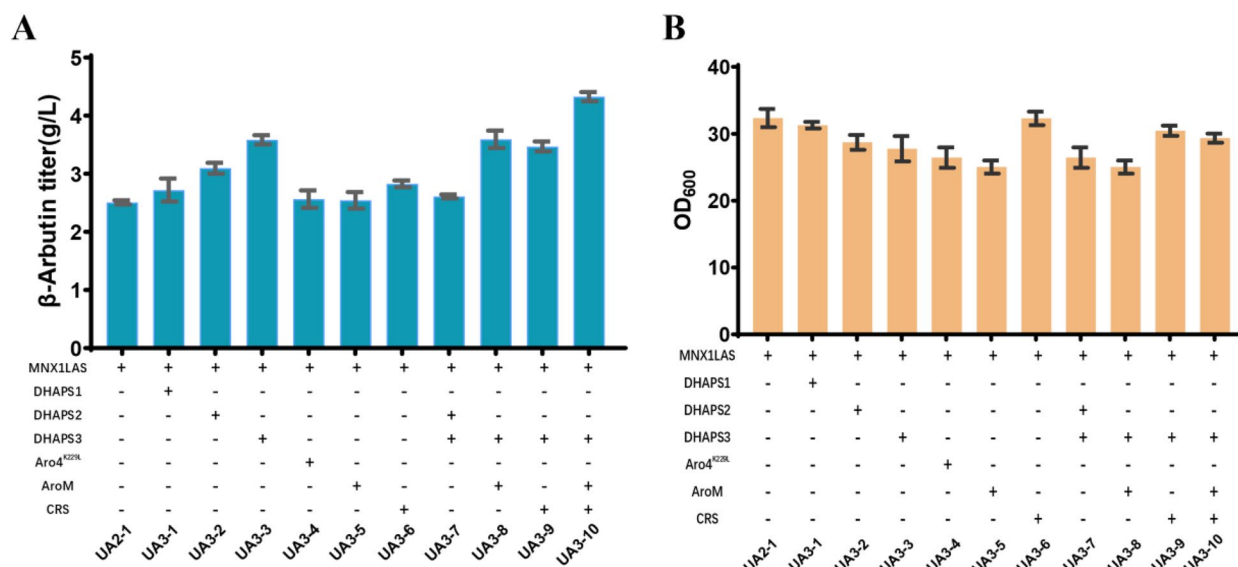


**Fig. 4** Influence of overexpressing related shikimate pathway genes on β-Arbutin production. **A** β-Arbutin titer and **B** OD<sub>600</sub> at 120 h. Data are presented as mean from triplicate experiments

and E4P to produce DHAP. Notably, the final step of the reaction catalyzed by AroM also utilizes PEP, indicating its continuous replenishment in shikimate pathway. Our objective is to boost PEP supply by knocking out pyruvate kinase (*Prk*, PAS\_chr2-1\_0769), overexpressing phosphoenolpyruvate carboxykinase (*Pyk*, PAS\_FragB\_0061) and the pyruvate carboxylase (*Pyc*, PAS\_chr2-2\_0024). To select the most effective strategy for increasing PEP supply, we initially selected UA2-1 as the chassis to validate these strategies

(Fig. 5A). Upon overexpressing *Pyk* or knocking out *Prk* in UA2-1, the β-Arbutin titer increased to a certain extent. Specifically, it reached 3.06 g/L in UA4-3 (22.2% higher than UA2-1) and 2.78 g/L in UA4-2 (11.0% higher than UA2-1). However, overexpression of *Pyc* only resulted in a β-Arbutin titer of 2.31 g/L, suggesting that overexpressing *Pyc* does not significantly impact the metabolic flux of PEP. Therefore, we overexpressed *Pyk* into UA3-10 (Fig. 5A). Surprisingly, this did not lead to an increase in β-Arbutin production in UA4-3.

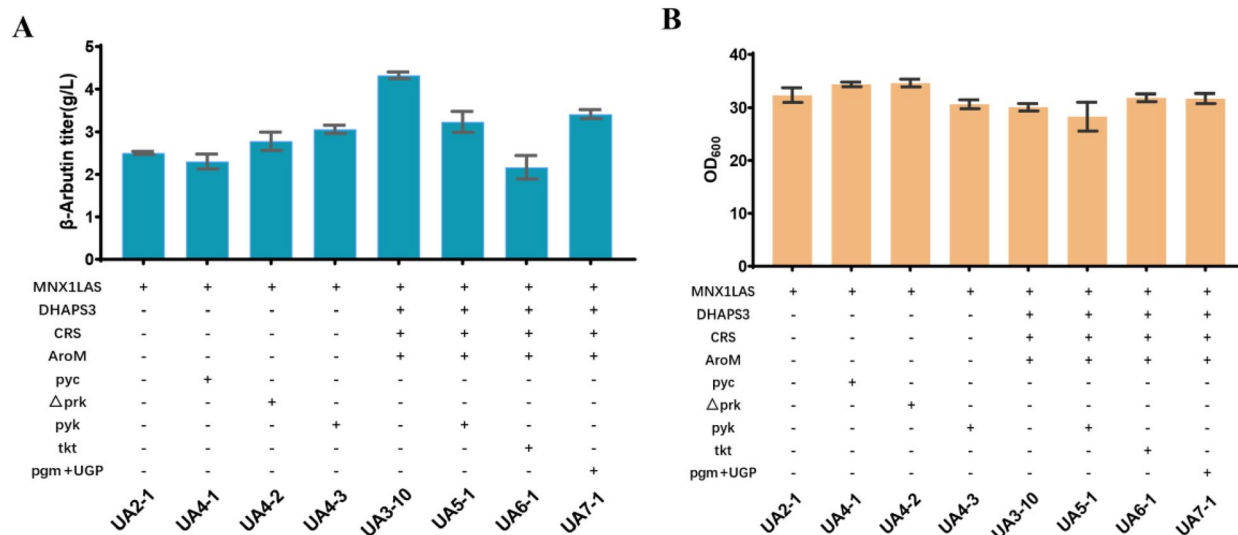


**Fig. 5** Increase the supply of precursors PEP, E4P and glucose donors UDPG to enhance the production of β-Arbutin. **A** β-Arbutin titer and **B** OD<sub>600</sub> at 120 h. Data are presented as mean from triplicate experiments



This indicates that although overexpression of *Pyk* helps to increase the metabolic flux of PEP, PEP itself is not currently the main limiting factor for increasing the  $\beta$ -Arbutin titer.

E4P is an intermediate in the PPP. According to metabolic flux analysis, the carbon flux available for E4P in yeast is estimated to be at least an order of magnitude lower than that of PEP [40]. Numerous studies have also confirmed that E4P is the primary limiting substrate and bottleneck for the biosynthesis of aromatic derivatives in various microbes [41–43]. To augment the production of aromatic compounds in yeast [33, 44, 45], studies have employed the strategy of overexpressing transketolase. The transketolase (*Tkt*, PAS\_chr1-4\_0150) facilitates the bypass of the oxidative phase of PPP, converting fructose-6-phosphate (F6P) and glyceraldehyde-3-phosphate (G3P) into E4P and xylulose-5-phosphate (Xu5P). Therefore, we overexpressed *Tkt* into UA3-10 to increase the supply of E4P. However, due to kinetic constraints inherent in the opposing reaction, the influence of *tkt* appears to be limited [33, 40, 44, 46, 47]. The titer of  $\beta$ -Arbutin exhibited a notable decrease (2.17 g/L), reflecting a reduction of 37.4% compared to the UA3-10 control (Fig. 5A), which may be correlated with the preference of *Tkt* for catalyzing the opposite reaction by consuming E4P [33]. This outcome aligns with findings similar to those reported by Liu [48].

UDPG plays a crucial role in the glucose transfer of  $\beta$ -Arbutin, representing the final step in its synthesis. In order to ensure sufficient availability of UDPG, we overexpressed the phosphoglucomutase (*Pgm*, PAS\_chr1-4\_0264) and UDP-glucose pyrophosphorylase (*UGP*, PAS\_chr1-3\_0122) in UA3-10, aiming to enhance the

conversion of G6P to UDPG. However, as shown in Fig. 5A, the  $\beta$ -Arbutin titer exhibited unfavorable change. This suggests that UDPG may not serve as a limiting factor in the production of  $\beta$ -Arbutin in UA3-10.

#### Optimizing methanol concentration to enhance the yield of $\beta$ -Arbutin

Methanol serves as the primary carbon source and inducer in the fermentation of most *K. phaffii*. Elevated methanol concentrations can result in the overproduction of formaldehyde, posing a risk of cell toxicity and disrupting normal growth and metabolism. Conversely, insufficient methanol levels can hinder characterization of the strain's production capacity. Therefore, precise regulation of methanol concentration during fermentation is crucial to promote optimal cell growth, metabolism, and production yield in *K. phaffii*. Various studies have investigated the impact of different methanol concentrations on the synthesis of recombinant proteins in methylotrophic yeast cells [49]. Consequently, it becomes essential to optimize methanol concentration for  $\beta$ -Arbutin production. To assess the growth and production capabilities of UA3-10 under varying methanol concentrations (1%, 1.5%, 2%, 2.5% and 3%), growth curves and  $\beta$ -Arbutin titers were measured (Fig. 6A, B). The results indicated that the maximum  $\beta$ -Arbutin titer was achieved at 2% methanol concentration. Specifically, at this concentration, strain UA3-10 produced 6.32 g/L of  $\beta$ -Arbutin, which is a 46.3% increase compared to 1% concentration. The OD<sub>600</sub> gradually increased with the rise in methanol concentration from 1 to 2%. However, beyond 2% methanol concentration, the  $\beta$ -Arbutin titer

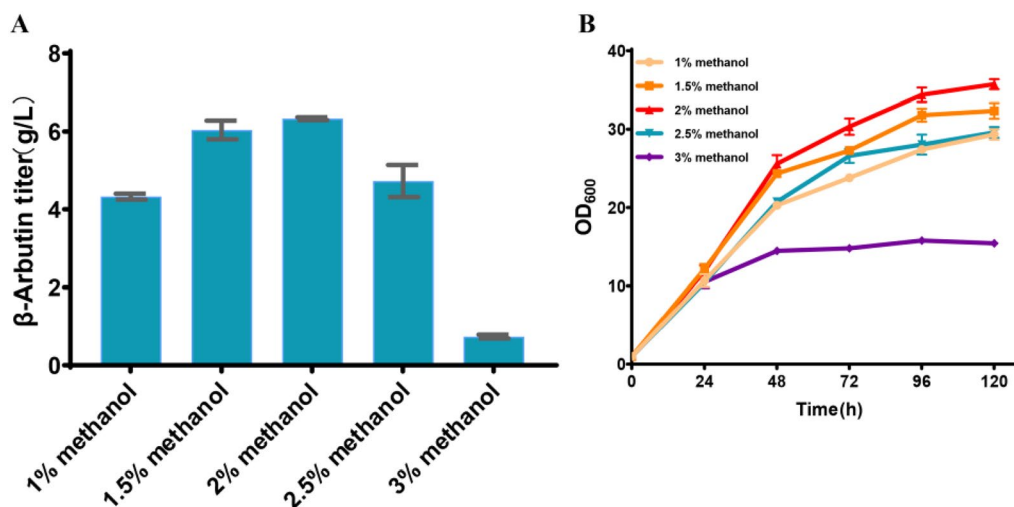


**Fig. 6** Effects of BMMY medium with different methanol concentrations per day on  $\beta$ -Arbutin production. **A** The  $\beta$ -Arbutin titers, and **B** growth curves of strain UA3-10 with different methanol concentrations. Data are presented as mean from triplicate experiments

showed no further increase. Moreover, at 3% methanol concentration, both  $OD_{600}$  and  $\beta$ -Arbutin titers sharply decreased, potentially attributed to the accumulation of methanol and formaldehyde [10, 50]. These findings highlight the importance of maintaining an appropriate methanol concentration for optimal  $\beta$ -Arbutin synthesis in *K. phaffii*. While increasing methanol supply at a suitable concentration enhances these processes, exceeding a certain threshold negatively affects growth and product synthesis adversely, and can even lead to cell death. It is noteworthy that methanol tolerance and bioconversion represent ongoing challenges in methylotrophic yeast biotransformation [10], necessitating further research.

#### Overexpression of heterologous PHK pathway to increase $\beta$ -Arbutin production

In order to identify the current bottleneck limiting  $\beta$ -Arbutin production, we overexpressed *UbiC* in the UA3-10 strain. Increasing precursor supply based on this approach may further enhance  $\beta$ -Arbutin production. Therefore, we further introduced the heterologous PHK (phosphoketolase) pathway to construct strain UA8-1.

As shown in Fig. 7, the production of  $\beta$ -Arbutin in UA8-1 showed an initial increase followed by a decrease, reaching the highest yield at 72 h, but only 1.25 g/L. The titer of  $\beta$ -Arbutin in UA8-1 is much lower than the control. Similar to increasing E4P supply by overexpress Tkt, the titer of  $\beta$ -Arbutin also suffered a significant decrease. The oxidative PPP is a major source of reductive power. Therefore, we speculate that the reason for the decrease in  $\beta$ -Arbutin production may be due to the introduction of the PHK pathway, which interferes with the generation of NADPH in the oxidative pentose phosphate pathway, thereby limiting the production of  $\beta$ -Arbutin. Therefore, using fructose-6-phosphate as the substrate to increase the supply of E4P may not be an

appropriate strategy for enhancing  $\beta$ -Arbutin production in *K. phaffii*. How to increase the supply of E4P without disrupting the normal reductive power supply of *K. phaffii* will be a question worth considering.

#### Scale-up production of $\beta$ -Arbutin

We conducted scale-up fermentation of UA3-10 in a 5 L fermenter and monitored  $OD_{600}$  and the  $\beta$ -Arbutin titer throughout the fermentation process (Fig. 8). To evaluate the performance of the optimal strain UA3-10, high-density fermentation was carried out in a 5 L fermenter, employing a fed-batch strategy. The two-stage fermentation process precisely controlled the carbon source for both cell growth and product accumulation. Upon culturing the strain for 18.6 h, glycerol in the BSM medium was depleted, initiating the glycerol fed-batch fermentation phase with a controlled flow rate at 5–10 g/h. After 32 h of cultivation,  $OD_{600}$  of the strain reached 278, prompting a 1-h pause in feeding. Following this starvation period, the methanol induction phase commenced. Initially, methanol was supplied at a flow rate of 5 g/h, with hourly interruptions in feeding to assess the methanol utilization ability of the strain. Monitoring DO changes within a minute helped prevent excessive methanol accumulation. As the strain adapted to the methanol flow rate, it was gradually increased, reaching a maximum flow rate of 20.7 g/h in this fermentation cycle. With the initiation of methanol feeding, there was a notable surge in  $\beta$ -Arbutin accumulation, while the increase in  $OD_{600}$  slowed down. Fermentation was terminated after 132 h of induction, with the maximum  $OD_{600}$  reaching 384 at 164 h. The peak production of  $\beta$ -Arbutin reached 128.6 g/L at 140 h, which was 1.89 times that of strain UA1-1 (68.02 g/L). The entire fermentation process, lasting 168 h, consumed 2996.8 g methanol, resulting in a total  $\beta$ -Arbutin yield of 501 g, with a volumetric productivity of 0.958 g/L h<sup>-1</sup>.

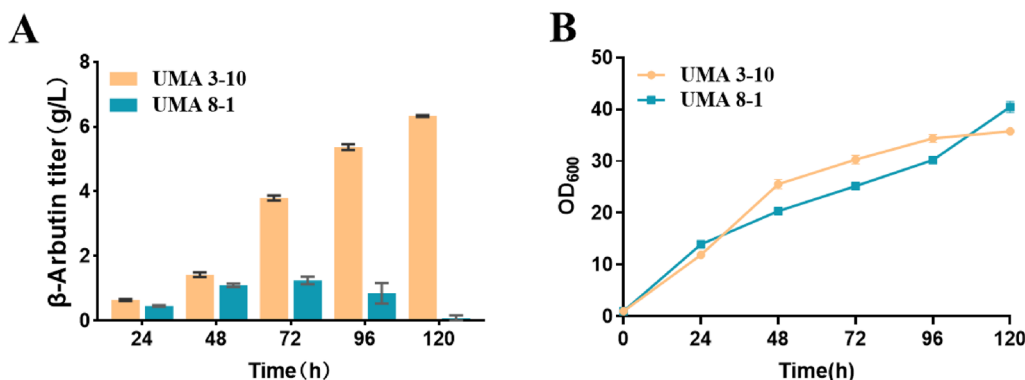


**Fig. 7** Effects of PHK pathway on the production of  $\beta$ -Arbutin. **A**  $\beta$ -Arbutin titer, and **B** growth curves of strains UA3-10 and UA8-1 with 2% methanol per day. Data are presented as mean from triplicate experiments

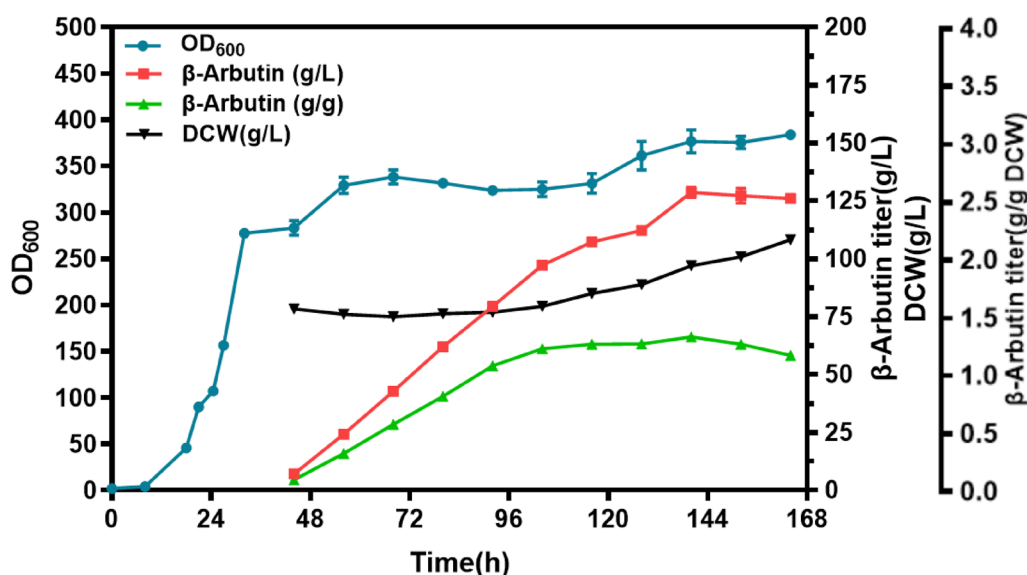


**Fig. 8** Production of  $\beta$ -Arbutin in fed-batch fermentation using the engineered strain UA3-10. The data are averages of 3 biological replicates with error bars representing standard deviations. Data are presented as mean from triplicate experiments

This achievement represents the highest titer reported using *K. phaffii*, surpassing other strains documented in the literature.

## Discussion

With the increasing demand for aromatic amino acid derivatives, utilizing recombinant microorganisms for fermentative production of aromatic amino acids and their derivatives is an effective way to meet the growing global demand. Taking  $\beta$ -Arbutin as an example, there have been multiple studies on its heterologous biosynthesis. Microbial production provides a promising approach for efficient and sustainable production of  $\beta$ -Arbutin. Shen et al. [21] successfully expressed the *MNX1* and *AS* in *E. coli* BL21Star (DE3), resulting in a synthetic pathway yielding 54.71 mg/L. Overexpression of the shikimate pathway genes increased the yield of  $\beta$ -Arbutin to 3.29 g/L. Shang et al. [4] achieved a  $\beta$ -Arbutin titer of 8.6 g/L by increasing the shikimate pathway flux and optimizing glucose concentrations. These studies primarily focused on the biosynthesis of target products in microorganisms with well-characterized model. In this study, we first established a biosynthetic pathway for  $\beta$ -Arbutin in *K. phaffii*. However, during the fermentation process for amplifying the production of  $\beta$ -Arbutin in strain UA1-1, it was observed that the culture medium gradually darkened, meaning the oxidation of the metabolic intermediate hydroquinone intensified with fermentation time. Utilizing *K. phaffii* for the production of  $\beta$ -Arbutin is complicated by the toxicity of intermediate metabolites, particularly on phenolic compounds (or

their oxidative products, such as benzoquinone), which negatively impacts the normal growth metabolism of the strain, thereby hindering the production of  $\beta$ -Arbutin. To address this, we constructed expression cassettes for the heterologous genes *UbiC*, *MNX1*, and *AS* using the inducible promoter AOX1. We employed a segmented fermentation strategy where glycerol served as the carbon source in the first phase, allowing for rapid microbial growth while preventing the expression of the three heterologous genes, thus avoiding any interference with cell growth. In the second phase, when methanol was introduced as the carbon source, expression of the three heterologous genes commenced, coinciding with the yeast having reached the logarithmic growth phase, thus possessing a favorable physiological state for the synthesis of  $\beta$ -Arbutin.

Due to the easy oxidation of hydroquinone, its oxidation product, benzoquinone, would impact the metabolic flux of hydroquinone towards  $\beta$ -Arbutin, thereby lowering the efficiency of  $\beta$ -Arbutin production. A gene fusion expression approach was adopted to incorporate the heterologous genes *MNX1* and *AS* to further enhance the yield of  $\beta$ -Arbutin. The fusion expression of genes *MNX1* and *AS* is being introduced and applied for the first time in the context of  $\beta$ -Arbutin production since the fermentation broth typically darkens to a rich brown color, indicative of benzoquinone formation. This coloration signifies severe oxidation of intermediate metabolites of phenolic compounds (with the oxidative product being benzoquinone), which adversely affects the metabolic flux of phenolic compounds

towards  $\beta$ -Arbutin synthesis. This issue is not occurred in other expression systems, making the fusion expression of *MNXI* and *AS* significantly impactful for yield enhancement in the biosynthesis of  $\beta$ -Arbutin in *K. phaffii*. Hence, an attempt was made to fuse the *MNXI* and *AS* enzymes using a short peptide linker GGGs. This fusion expression in the strain UA2-1 yielded a  $\beta$ -Arbutin concentration of 1.88 g/L, which was 19.7% higher compared to strain UA1-1. This proves that the fused protein *MNXI*-GGGS-*AS* is advantageous for the synthesis of  $\beta$ -Arbutin. It laid the foundation for subsequent pathway improvements.

Overexpression of rate-limiting enzymes is often employed to regulate metabolic pathways and enhance engineered strain biosynthesis [51]. To improve the yield of synthesizing  $\beta$ -Arbutin, we implemented a rate-limiting gene screening and iterative gene assembly strategy to screen and enhance the expression of rate-limiting enzymes. Overexpression of *DHAPS1*, *DHAPS2*, *DHAPS3*, *AroM*, *CRS* and *Aro4<sup>K229L</sup>* were individually carried out, followed by combinatorial overexpression upon identification of effective genes. Conceptually, each gene was individually overexpressed, observing its disturbance on  $\beta$ -Arbutin synthesis to determine the yeast system's sensitivity to enzyme requirements. The results indicated that the assembly of overexpressed *DHAPS3*, *CRS*, and *AroM* can significantly increase the synthesis of  $\beta$ -Arbutin, reaching 1.72 times that of the UA2-1 strain. This approach can also be used to improve the synthesis of other compounds in shikimate pathway in *K. phaffii*.

In the following, attempts were made to increase the concentration of  $\beta$ -Arbutin by enhancing the precursors. In order to accumulate the precursor PEP, the *Pyk* gene was overexpressed. While this was advantageous for increasing the metabolic flux of PEP, it was not a significant limiting factor for  $\beta$ -Arbutin titer in UA3-10. To identify the limiting factors of  $\beta$ -Arbutin titer in UA3-10, efforts were made to increase the supply of E4P by overexpressing *Tkt*. However, the titer of  $\beta$ -Arbutin decreased instead, suggesting a possible association with the preference of *Tkt* for catalyzing the reverse reaction by consuming E4P. This finding is consistent with the results reported by Liu et al [48]. The PHK pathway was subsequently confirmed as an effective strategy to boost E4P supply [48]. Despite overexpressing *UbiC* and introducing the PHK pathway to enhance E4P supply, the yields remained decreased. The oxidative ppp is a major source of reducing power and metabolic intermediates in biosynthetic processes [52]. Therefore, we speculate that the introduction of the PHK pathway, disrupting the generation of NADPH in the ppp, may be the reason for the decrease in  $\beta$ -Arbutin titer. The expression of *Pgm* and *UGP* is an effective strategy to increase UDPG supply in

yeast [7]. We also confirmed that UDPG is not a limiting factor for the  $\beta$ -Arbutin titer in strain UA3-10 through the overexpression of endogenous *Pgm* and *UGP* genes to attempt to increase the supply of UDPG. What are the limiting factors that affect the synthesis of  $\beta$ -Arbutin in UA3-10 is a question that is worth considering.

Precise regulation of methanol concentration during fermentation is crucial to promote optimal cell growth, metabolism, and production yield in *K. phaffii* [49]. After optimizing methanol concentration to 2% methanol per day, the production of  $\beta$ -Arbutin reached 6.32 g/L in shake flask after 120 h. In the end, we conducted high-density fermentation of the UA3-10 strain in a 5 L fermenter, achieving a  $\beta$ -Arbutin yield of 128.6 g/L. The results of this study will serve as a valuable resource for future research on the production of derivatives of shikimate pathway. Furthermore, this work has made significant contributions to the existing  $\beta$ -Arbutin synthesis. We have further overexpressed the heterologous pathway genes. Following the overexpression of *UbiC*, the yield of  $\beta$ -Arbutin increased to 7.29 g/L (data not shown), indicating that the metabolic flux of chorismate significantly impacts the production of  $\beta$ -Arbutin. Our next step is to perform knockouts on the branch pathways of the shikimate pathway, targeting genes such as chorismate mutase, prephenate dehydratase, prephenate dehydrogenase, and anthranilate synthase for either individual or combinatorial knockouts. After enhancing NADPH supply, we will reassemble the PHK pathway. This is the regulatory strategy we are currently preparing to implement. Looking ahead, we plan to explore various engineering strategies to further enhance the synthetic efficiency of *K. phaffii* and expand the potential applications of  $\beta$ -Arbutin.

## Conclusions

Using a yeast cell factory, we demonstrated a strategy for the efficient assembly and regulation to the biosynthetic pathway for  $\beta$ -Arbutin.  $\beta$ -Arbutin production was significantly enhanced by combining comprehensive strategies, including fusion protein construction, enhancing shikimate pathway flux, and augmenting precursor supplies (PEP, E4P, and UDPG). The  $\beta$ -Arbutin yield in the best-performing recombinant strain, UA3-10, reached 6.32 g/L, representing threefold enhancement compared to the strain UA1-1 using the simple assembly pathway. The peak production of  $\beta$ -Arbutin in UA3-10 reached 128.6 g/L, which represents the highest titer reported using *K. phaffii*, surpassing other strains to our knowledge. This study provides an effective scheme for regulating heterologous  $\beta$ -Arbutin pathways in

yeast, offering a green and cost-effective alternative that can be applied to the efficient synthesis of  $\beta$ -Arbutin in microbial cells.

#### Abbreviations

<i>UbiC</i>	Chorismate lyase
<i>MNX1</i>	4-Hydroxybenzoate 1-hydroxylase
<i>AS</i>	Arbutin synthase
<i>Pyk</i>	Phosphoenolpyruvate carboxykinase
<i>Prk</i>	Pyruvate kinase
<i>Pyc</i>	Pyruvate carboxylase
<i>DHAPS</i>	3-Deoxy-7-Phosphoheptulonate synthase
<i>AroM</i>	Pentafunctional AROM polypeptide
<i>CRS</i>	Chorismate synthase
<i>Tkt</i>	Transaldolase
<i>Pgm</i>	Phosphoglucomutase
<i>UGP</i>	UDP-glucose pyrophosphorylase
<i>Xfpk</i>	Phosphoketolase
<i>PTA</i>	Phosphate acetyltransferase
<i>Xu5P</i>	Xylulose 5-Phosphate
<i>PPP</i>	Pentose phosphate pathway

#### Supplementary Information

The online version contains supplementary material available at <https://doi.org/10.1186/s12934-024-02525-8>.

**Additional file 1.** Strains, plasmids, and primers used in this study (Table S1). HPLC analysis of 0.2 g/L  $\beta$ -Arbutin standard and the supernatant of strain UA1-1 fermentation. The red curve represents the peak chart of  $\beta$ -Arbutin standard, while the black curve represents the fermentation supernatant of UA1-1 (Figure S1). Growth curve and the  $\beta$ -Arbutin titer of strain UA1-1 during methanol induction stage in fed-batch fermentation (Figure S2).

#### Acknowledgements

Not applicable.

#### Author contributions

JY performed the experiments and analyzed the data this work. LY, FZ, CY, SH supported the experiments and discussions. SH guided the research throughout the whole process. She provided support in manuscript revision and offered valuable suggestions. LY and FZ conceived and supervised the research. All authors read and approved the final manuscript.

#### Funding

This work was supported by the National Key R&D Program of China [2018YFA0901500].

#### Data availability

The datasets used and/or analysed during the current study are available from the corresponding author on reasonable request.

#### Declarations

#### Ethics approval and consent to participate

Not applicable.

#### Consent for publication

Not applicable.

#### Competing interests

The authors declare that they have no competing interests.

#### Author details

<sup>1</sup>Guangdong Key Laboratory of Fermentation and Enzyme Engineering, School of Biology and Biological Engineering, South China University of Technology, Guangzhou 510006, People's Republic of China.

Received: 9 July 2024 Accepted: 9 September 2024

Published online: 30 September 2024

#### References

- Guo Jing Xu, Ping JL. Research progress of arbutin. *Ningxia Med J.* 2008;30(3):281–3. <https://doi.org/10.3969/j.issn.1001-5949.2008.03.050>.
- Dong-Seok Kim D-SK, Hailan Li HL, Yun-Mi Jeong Y-MJ, et al. Arbutin inhibits TCCSUP human bladder cancer cell proliferation via up-regulation of P21. *Pharmazie.* 2011;66(4):306–9. <https://doi.org/10.1691/ph.2011.0785>.
- Lee H-J, Kim K-W. Anti-inflammatory effects of arbutin in lipopolysaccharide-stimulated BV2 microglial cells. *Inflamm Res.* 2012;61(8):817–25. <https://doi.org/10.1007/s00011-012-0474-2>.
- Shang Y, Wei W, Zhang P, Ye B-C. Engineering *Yarrowia lipolytica* for enhanced production of arbutin. *J Agric Food Chem.* 2020;68(5):1364–72. <https://doi.org/10.1021/acs.jafc.9b07151>.
- Xu K-X, Xue M-G, Li Z, Ye B-C, Zhang B. Recent progress on feasible strategies for arbutin production. *Front Bioeng Biotechnol.* 2022;10:914280. <https://doi.org/10.3389/fbioe.2022.914280>.
- Zhu S. Extraction and purification of  $\beta$ -arbutin from pear leaves and study on the characteristics of phospholipid complex. *Beijing For Univ.* 2021. <https://doi.org/10.26949/d.cnki.gblyu.2021.000334>.
- An N, Xie C, Zhou S, Wang J, Sun X, Yan Y, Shen X, Yuan Q. Establishing a growth-coupled mechanism for high-yield production of  $\beta$ -Arbutin from glycerol in *Escherichia coli*. *Bioresour Technol.* 2023;369:128491. <https://doi.org/10.1016/j.biortech.2022.128491>.
- Espinosa MI, Gonzalez-Garcia RA, Valgepea K, Plan MR, Scott C, Pretorius IS, Marcellin E, Paulsen IT, Williams TC. Adaptive laboratory evolution of native methanol assimilation in *Saccharomyces cerevisiae*. *Nat Commun.* 2020;11(1):5564. <https://doi.org/10.1038/s41467-020-19390-9>.
- Woolston BM, King JR, Reiter M, Van Hove B, Stephanopoulos G. Improving formaldehyde consumption drives methanol assimilation in engineered *E. coli*. *Nat Commun.* 2018;9(1):2387. <https://doi.org/10.1038/s41467-018-04795-4>.
- Cai P, Wu X, Deng J, Gao L, Shen Y, Yao L, Zhou YJ. Methanol biotransformation toward high-level production of fatty acid derivatives by engineering the industrial yeast *Pichia pastoris*. *Proc Natl Acad Sci.* 2022;119(29):e2201711119. <https://doi.org/10.1073/pnas.2201711119>.
- Bernauer L, Radkohl A, Lehmayr LGK, Emmerstorfer-Augustin A. *Komagataella phaffii* as emerging model organism in fundamental research. *Front Microbiol.* 2021;11:607028. <https://doi.org/10.3389/fmicb.2020.607028>.
- Ejike UC, Chan CJ, Lim CSY, Lim RLH. Functional evaluation of a recombinant fungal immunomodulatory protein from *L. rhinoceros* produced in *P. pastoris* and *E. coli* host expression systems. *Appl Microbiol Biotechnol.* 2021;105(7):2799–813. <https://doi.org/10.1007/s00253-021-11225-x>.
- Ahmad M, Hirz M, Pichler H, Schwab H. Protein expression in *Pichia pastoris*: recent achievements and perspectives for heterologous protein production. *Appl Microbiol Biotechnol.* 2014;98(12):5301–17. <https://doi.org/10.1007/s00253-014-5732-5>.
- Küberl A, Schneider J, Thallinger GG, Anderl I, Wibberg D, Hajek T, Jaenicke S, Brinkrolf K, Goesmann A, Szczepanowski R, Pühler A, Schwab H, Glieder A, Pichler H. High-quality genome sequence of *Pichia pastoris* CBS7435. *J Biotechnol.* 2011;154(4):312–20. <https://doi.org/10.1016/j.jbiotec.2011.04.014>.
- Sturmberger L, Chappell T, Geier M, Krainer F, Day KJ, Vide U, Trstenjak S, Schiefer A, Richardson T, Soriaga L, Darnhofer B, Birner-Gruenberger R, Glick BS, Tolstorukov I, Cregg J, Madden K, Glieder A. Refined *Pichia pastoris* reference genome sequence. *J Biotechnol.* 2016;235:121–31. <https://doi.org/10.1016/j.jbiotec.2016.04.023>.
- Fischer JE, Glieder A. Current advances in engineering tools for *Pichia pastoris*. *Curr Opin Biotechnol.* 2019;59:175–81. <https://doi.org/10.1016/j.copbio.2019.06.002>.
- Qian D, Zhang C, Deng C, Zhou M, Fan L, De ZL. Novo biosynthesis of 2'-fucosyllactose in engineered *Pichia pastoris*. *Biotechnol Lett.* 2023;45(4):521–36. <https://doi.org/10.1007/s10529-023-03357-z>.

18. Siebert M, Severin K, Heide L. Formation of 4-Hydroxybenzoate in *Escherichia coli* characterization of the ubiC gene and its encoded enzyme chorismate pyruvate-lyase. *Microbiology*. 1994;140(4):897–904.
19. Eppink MH, Boeren SA, Vervoort J, Van Berkel WJ. Purification and properties of 4-hydroxybenzoate 1-hydroxylase (decarboxylating), a novel flavin adenine dinucleotide-dependent monooxygenase from *Candida parapsilosis* CBS604. *J Bacteriol*. 1997;179(21):6680–7. <https://doi.org/10.1128/jb.179.21.6680-6687.1997>.
20. Arend J, Warzecha H, Hefner T, Stöckigt J. Utilizing genetically engineered bacteria to produce plant-specific glucosides: engineered bacteria to produce plant-specific glucosides. *Biotechnol Bioeng*. 2001;76(2):126–31. <https://doi.org/10.1002/bit.1152>.
21. Shen X, Wang J, Wang J, Chen Z, Yuan Q, Yan Y. High-level de novo biosynthesis of arbutin in engineered *Escherichia coli*. *Metab Eng*. 2017;42:52–8. <https://doi.org/10.1016/j.ymben.2017.06.001>.
22. Wang S, Fu C, Bilal M, Hu H, Wang W, Zhang X. Enhanced biosynthesis of arbutin by engineering shikimate pathway in pseudomonas chlororaphis P3. *Microb Cell Factories*. 2018;17(1):174. <https://doi.org/10.1186/s12934-018-1022-8>.
23. An N, Zhou S, Chen X, Wang J, Sun X, Shen X, Yuan Q. High-yield production of  $\beta$ -Arbutin by identifying and eliminating byproducts formation. *Appl Microbiol Biotechnol*. 2023;107(20):6193–204. <https://doi.org/10.1007/s00253-023-12706-x>.
24. Gibson DG. Enzymatic assembly of overlapping DNA fragments. In: *Methods in Enzymology*, vol. 498. Elsevier, 2011. p. 349–61. <https://doi.org/10.1016/B978-0-12-385120-8.00015-2>.
25. Wu S, Letchworth GJ. High efficiency transformation by electroporation of *Pichia pastoris* pretreated with lithium acetate and dithiothreitol. *Biotechniques*. 2004;36(1):152–4. <https://doi.org/10.2144/04361DD02>.
26. Li C, Lin Y, Zheng X, Yuan Q, Pang N, Liao X, Huang Y, Zhang X, Liang S. Recycling of a selectable marker with a self-excisable plasmid in *Pichia pastoris*. *Sci Rep*. 2017;7(1):11113. <https://doi.org/10.1038/s41598-017-11494-5>.
27. Gao J, Xu J, Zuo Y, Ye C, Jiang L, Feng L, Huang L, Xu Z, Lian J. Synthetic biology toolkit for marker-less integration of multigene pathways into *Pichia pastoris* via CRISPR/Cas9. *ACS Synth Biol*. 2022;11(2):623–33. <https://doi.org/10.1021/acssynbio.1c00307>.
28. Kong X, He Q, Yue A, Wu S, Li J. Determination of arbutin in apple juice concentrate by ultra performance liquid chromatography with electrospray ionization tandem mass spectrometry: determination of arbutin in apple juice concentrate by ultra performance liquid chromatography with electrospray ionization tandem mass spectrometry. *Chin J Chromatogr*. 2010;28(6):632–4. <https://doi.org/10.3724/SP.J.1123.2010.00632>.
29. Huxia, Chenminglong, Yangweihan, et al. Determination of arbutin in soluble microneedle patches by HPLC. *J Shanxi Med Univ*. 2018;49(5): 4. <https://doi.org/10.13753/j.issn.1007-6611.2018.05.009>.
30. Jiang G-Z, Yao M-D, Wang Y, Zhou L, Song T-Q, Liu H, Xiao W-H, Yuan Y-J. Manipulation of GES and ERG20 for geraniol overproduction in *Saccharomyces cerevisiae*. *Metab Eng*. 2017;41:57–66. <https://doi.org/10.1016/j.ymben.2017.03.005>.
31. Hu T, Zhou J, Tong Y, Su P, Li X, Liu Y, Liu N, Wu X, Zhang Y, Wang J, Gao L, Tu L, Lu Y, Jiang Z, Zhou YJ, Gao W, Huang L. Engineering chimeric diterpene synthases and isoprenoid biosynthetic pathways enables high-level production of miltiradiene in yeast. *Metab Eng*. 2020;60:87–96. <https://doi.org/10.1016/j.ymben.2020.03.011>.
32. Hartmann M, Schneider TR, Pfeil A, Heinrich G, Lipscomb WN, Braus GH. Evolution of feedback-inhibited  $\beta/\alpha$  barrel isoenzymes by gene duplication and a single mutation. *Proc Natl Acad Sci*. 2003;100(3):862–7.
33. Curran KA, Leavitt JM, Karim AS, Alper HS. Metabolic engineering of muconic acid production in *Saccharomyces cerevisiae*. *Metab Eng*. 2013;15:55–66. <https://doi.org/10.1016/j.ymben.2012.10.003>.
34. Li M, Kildegaard KR, Chen Y, Rodriguez A, Borodina I, De NJ. Novo production of resveratrol from glucose or ethanol by engineered *Saccharomyces cerevisiae*. *Metab Eng*. 2015;32:1–11. <https://doi.org/10.1016/j.ymben.2015.08.007>.
35. Suastegui M, Matthiesen JE, Carraher JM, Hernandez N, Rodriguez Quiroz N, Okerlund A, Cochran EW, Shao Z, Tessonnier J. Combining metabolic engineering and electrocatalysis: application to the production of polyamides from sugar. *Angew Chem Int Ed*. 2016;55(7):2368–73. <https://doi.org/10.1002/anie.201509653>.
36. Duncan K, Edwards RM, Coggins JR. The pentafunctional *arom* enzyme of *Saccharomyces cerevisiae* is a mosaic of monofunctional domains. *Biochem J*. 1987;246(2):375–86. <https://doi.org/10.1042/bj2460375>.
37. Mao J, Liu Q, Song X, Wang H, Feng H, Xu H, Qiao M. Combinatorial analysis of enzymatic bottlenecks of L-tyrosine pathway by p-coumaric acid production in *Saccharomyces cerevisiae*. *Biotechnol Lett*. 2017;39(7):977–82. <https://doi.org/10.1007/s10529-017-2322-5>.
38. Luo G, Lin Y, Chen S, Xiao R, Zhang J, Li C, Sinskey AJ, Ye L, Liang S. Overproduction of patchoulol in metabolically engineered *Komagataella phaffii*. *J Agric Food Chem*. 2023;71(4):2049–58. <https://doi.org/10.1021/acs.jafc.2c08228>.
39. Zhang X, Chen S, Lin Y, Li W, Wang D, Ruan S, Yang Y, Liang S. Metabolic engineering of *Pichia pastoris* for high-level production of lycopene. *ACS Synth Biol*. 2023;12(10):2961–72. <https://doi.org/10.1021/acssynbio.3c00294>.
40. Suástegui M, Guo W, Feng X, Shao Z. Investigating strain dependency in the production of aromatic compounds in *Saccharomyces cerevisiae*. *Biotechnol Bioeng*. 2016;113(12):2676–85. <https://doi.org/10.1002/bit.26037>.
41. Ikeda M. Towards bacterial strains overproducing L-tryptophan and other aromatics by metabolic engineering. *Appl Microbiol Biotechnol*. 2006;69(6):615–26. <https://doi.org/10.1007/s00253-005-0252-y>.
42. Flores N, Xiao J, Berry A, Bolivar F, Valle F. Pathway engineering for the production of aromatic compounds in *Escherichia coli*. *Nat Biotechnol*. 1996;14:620–3.
43. Patnaik R, Liao JC. Engineering of *Escherichia coli* central metabolism for aromatic metabolite production with near theoretical yield. *Appl Environ Microbiol*. 1994;60(11):3903–8. <https://doi.org/10.1128/aem.60.11.3903-3908.1994>.
44. Suástegui M, Yu Ng C, Chowdhury A, Sun W, Cao M, House E, Maranas CD, Shao Z. Multilevel engineering of the upstream module of aromatic amino acid biosynthesis in *Saccharomyces cerevisiae* for high production of polymer and drug precursors. *Metab Eng*. 2017;42:134–44. <https://doi.org/10.1016/j.ymben.2017.06.008>.
45. Carly F, Vandermies M, Telek S, Steels S, Thomas S, Nicaud J-M, Fickers P. Enhancing erythritol productivity in *Yarrowia lipolytica* using metabolic engineering. *Metab Eng*. 2017;42:19–24. <https://doi.org/10.1016/j.ymben.2017.05.002>.
46. Deaner M, Alper HS. Systematic testing of enzyme perturbation sensitivities via graded dCas9 modulation in *Saccharomyces cerevisiae*. *Metab Eng*. 2017;40:14–22. <https://doi.org/10.1016/j.ymben.2017.01.012>.
47. Sprenger GA, Schörken U, Sprenger G, Sahn H. Transketolase of *Escherichia coli* K12: purification and properties of the enzyme from recombinant strains. *Eur J Biochem*. 1995;230(2):525–32. <https://doi.org/10.1111/j.1432-1033.1995.0525hx>.
48. Liu Q, Yu T, Li X, Chen Y, Campbell K, Nielsen J, Chen Y. Rewiring carbon metabolism in yeast for high level production of aromatic chemicals. *Nat Commun*. 2019;10(1):4976. <https://doi.org/10.1038/s41467-019-12961-5>.
49. Karbalaee M, Rezaee SA, Farsiani H. *Pichia pastoris*: a highly successful expression system for optimal synthesis of heterologous proteins. *J Cell Physiol*. 2020;235(9):5867–81. <https://doi.org/10.1002/jcp.29583>.
50. Chen FY-H, Jung H-W, Tsuei C-Y, Liao JC. Converting *Escherichia coli* to a synthetic methylotroph growing solely on methanol. *Cell*. 2020;182(4):933-946.e14. <https://doi.org/10.1016/j.cell.2020.07.010>.
51. Cravens A, Payne J, Smolke CD. Synthetic biology strategies for microbial biosynthesis of plant natural products. *Nat Commun*. 2019;10(1):2142. <https://doi.org/10.1038/s41467-019-09848-w>.
52. Kruger NJ, Von Schaewen A. The oxidative pentose phosphate pathway: structure and organisation. *Curr Opin Plant Biol*. 2003;6(3):236–46. [https://doi.org/10.1016/S1369-5266\(03\)00039-6](https://doi.org/10.1016/S1369-5266(03)00039-6).

## Publisher's Note

Springer Nature remains neutral with regard to jurisdictional claims in published maps and institutional affiliations.